Preventive Dispatch Against Attack of Adjustable Load on Power System Frequency

Yuan Zhang, *Graduate Student Member*, *IEEE*, Mingxu Xiang, *Member*, *IEEE*, Zhengwen Huang, *Member*, *IEEE*, and Zhifang Yang, *Senior Member*, *IEEE*

***Abstract*—With the increase of adjustable loads connected to power systems, there is a growing risk of intentionally exploiting load adjustability to cause power balance deviations. This poses an obvious threat to power system frequency, which has been noticed by many system operators. However, the current dispatch method cannot consider the attack of load on frequency, let alone providing a preventive dispatch decision that reduces the frequency deviation. To address this challenge, a preventive dispatch method that mitigates the impact of adjustable load on power system frequency is presented for the first time. The relationship between the time-varying power mismatch caused by the attack of adjustable load and frequency deviation is established. This is achieved by theoretically deriving the transfer function between system frequency and power mismatch in time domain and discretizing the function into several segments according to the division of time horizons. A formal analysis of the error caused by the transformation is performed, which provides quantitative guidance on the accuracy of the frequency modeling. Based on this, the worst-case scenario of frequency deviation with adjustable load is determined through solving an optimization model. Then, a novel preventive dispatch method that guarantees the system frequency security under the worst-case scenario is presented. Particularly, the generator ramping behavior after receiving the AGC adjustment command is modeled by a group of linear constraints to distinguish the load tracking abilities of generators. Case studies based on the IEEE30-bus system and a 661-bus utility system show that the proposed preventive dispatch method can achieve a 5.8%–19.42% improvement of the maximum absolute frequency deviation.**

***Index Terms*—Adjustable load, time varying power mismatch, power system frequency, dispatch model, generator ramping.**

I. Introduction

Power balance between generation and load in modern power systems is challenging because of the increasing fluctuations. It has been widely recognized by power system operators around the world that it is necessary to utilize the flexibility of loads as a supplement for the generation side. Since the concept of demand response is proposed in the 1980s [1], its benefits have been appreciated at different time scales of power system operation [2], [3].

However, while providing flexibility, adjustable loads also pose a threat to power balance if the load control system is attacked and monitored against the stable operation [4]. Considering that loads are connected to the power grid in a distributed manner with imperfect cyber-attack defense system, the risk that the adjustability of the loads is utilized on purpose to create deviations of power balance is much higher than the generation side [5], [6]. Especially with the increase of smart devices, including electric vehicle chargers and intelligent air conditioners, the influence of adjustable loads on system operation security has gained the attention in many countries [7]–[9]. Investigations have performed in many power grids to ensure stable power system operation when a large scale of load is purposely adjusted [10], [11]. For example, in 2020, during extreme heatwaves, rapid surges in air conditioning loads (similar to a coordinated load attack) pushed the California grid to its limits. To prevent frequency collapse, CAISO imposed rolling blackouts, causing grave damage to people's lives. Centralized control systems for clustered air conditioning units provide a potential attack vector for malicious actors to manipulate load profiles remotely.

Power mismatch caused by the deliberate adjustment of loads has an obvious influence on system frequency. Within the scheduling period, the intended load change can cause a shortage of frequency regulation ability, leading to unsafe frequency changes. For example, studies have shown that a 30% increase in demand can

Received: April 5, 2025
Accepted: December 3, 2025
Published Online: March 1, 2026

Yuan Zhang, Mingxu Xiang (corresponding author), and Zhifang Yang are with the State Key Laboratory of Power Transmission Equipment Technology, the School of Electrical Engineering, Chongqing University, Chongqing, 400044, China (e-mail: 20173593@cqu.edu.cn; mxxiang@cqu.edu.cn; zfyang@cqu.edu.cn).

Zhengwen Huang is with the Department of Electronic and Electrical Engineering, College of Engineering, Design & Physical Sciences, Brunel University London, Uxbridge UB8 3PH, UK (e-mail: Zhengwen.Huang@brunel.ac.uk).

DOI: 10.23919/PCMP.2024.000463

result in tripping of all the generators on the power grid model of the Western System Coordinating Council and cause frequency instability in the system [12]. Also, with the increasing integration of aggregated flexible loads, the power grids in China are also concerned about the frequency fluctuations caused by load disturbances, especially the platform that gathers a large number of loads (like the intelligent air conditioner control system). However, most current research focuses on identifying or resolving network attacks from the perspective of information protection and communication systems. There still lacks a formal quantitative analysis on to what extent that adjustable load can threaten the frequency and how to schedule the generators against such risks. To solve this, two prospects are required.

1) The determination of the worst scenario associated with the maximum frequency deviation facing time-varying power mismatch caused by the adjustable load. It requires establishing the relationship between time-varying power mismatch and the frequency deviation in an analytical form. Also, the potential frequency deviation at different time scales is required.

2) The modeling of system response behavior facing the frequency deviations caused by the adjustable load. It needs to formulate the adjustment of generators governed by the automatic generation control (AGC) system when frequency deviation occurs. This modeling provides the basis for the preventative dispatch that aims at controlling the frequency deviation.

A. Frequency Deviation Giving Time-varying Power Mismatch

In the power system scheduling problem, it is difficult to directly obtain the analytical form of the frequency security constraints due to the nonlinear and high-order feature of the relationship between frequency and power mismatch [13]. Simplifications are required to provide a tractable expression of the frequency security constraints in the dispatch problem. Basically, there are two types of frequency modeling facing power mismatch.

The first type is the frequency modeling after a large power mismatch. Relative studies normally focus on the frequency nadir or rate of change of frequency (RoCoF) after a given power mismatch, such as when a large and sudden generation infeed loss occurs [14], [15]. Studies have shown that an approximate analytical expression of frequency dynamics can be deduced by simplifying the governor characteristics of the generator and neglecting the effect of load damping [16]. The excessive RoCoF and frequency nadir can be handled by the coordination of the control parameters of inertia response [17] or energy storage [18], [19].

Though the basic frequency response model is well-established in existing power system analysis, in this paper, we are mainly interested in the quasi-steady frequency deviation given the time-varying power mismatch. It can be regarded as the frequency deviation value after the time approaches infinity for the aforementioned type of frequency dynamic modeling. Essentially, the quasi-steady state frequency behavior can be regarded as an integral transfer function of the power mismatch, where the transfer function describes the relationship between the power change, corresponding to a net load change, and frequency deviation [20]. By neglecting the time response, existing studies widely acknowledge that the frequency deviation is proportional to the power mismatch according to the primary frequency response characteristics. In [21], the constraints on the frequency deviation are modeled in the dispatch problem to ensure a secure system operation. However, the accuracy of this modeling is not verified. Especially, when determining the frequency deviation influenced by the adjustable load, the potential frequency at each time step needs to be compared. However, such a method is still not reported in existing methods.

B. System Response Behavior Facing Frequency Deviation

When a large frequency deviation appears, the system frequency response mechanism will be activated. First, the primary frequency reserve (PFR) will be effective, which is typically achieved by the turbine-governor response and is an autonomous response by the built-in governor in the generator. Then, the frequency deviation will be further corrected by the deployment of the secondary frequency reserve, which is typically deployed by AGC [22]. The AGC system will be active when the frequency deviation exceeds the tolerance, and generators will adjust to mitigate the power mismatch and pull the frequency to the normal level [17]. Many system operators co-optimize the energy dispatch and frequency reserve to ensure sufficient adjustability facing frequency deviation [23]. In real time, the regulation reserve is deployed by AGC to balance generation and load every several seconds under normal operation conditions. Existing studies have shown that the detailed modeling of AGC actions in the dispatch problem can lead to an improvement of frequency performance, even considering the forecast difficulties of the high-resolution demand curve [24], [25]. The regulation adjustment is modeled, and the allocation of the adjustment to different frequency regulation resources is proposed in [26]–[28]. When the system faces large fluctuations, the detailed modeling of AGC actions in the dispatch problem can ensure that the power system is more prepared for the frequency response.

However, existing methods still cannot capture the different ramping abilities of generators when incorporating the AGC actions in the dispatch model. When considering the attack of adjustable load on the system

frequency, it is important to prepare flexible resources to track the deviation of the load. This problem will be addressed in this paper.

C. Contributions of This Work

To deal with the aforementioned issues, the paper aims to evaluate the threat of adjustable load on power system frequency and develop a preventive dispatch method to ensure a secure operation. The contributions of this work are summarized as follows.

1) The worst-case scenario determination for frequency deviations caused by a load attack is formally formulated. Deriving the transfer function between the time-varying power mismatch and frequency in time domain, the frequency expression considering time-varying adjustable load is established. Based on this, a group of load attack scenarios with the largest frequency deviation at each scheduling time is obtained, from which the worst scenario across multiple dispatch intervals is determined, which is absent in conventional frequency security frameworks.

2) A preventive dispatch model considering the worst-case scenario of frequency deviation is proposed. In this model, the different behaviors of the generators ramping after receiving the AGC adjustment command is modeled by a group of linear constraints to distinguish the load tracking abilities of generators. Then, a mixed-integer linear programming (MILP) problem is formulated to reduce the maximum potential frequency deviation.

The validity of this method is demonstrated by testing on the IEEE30-bus system and a 661-bus utility system. The results indicate that the proposed preventive dispatch method achieves performance improvement of at least 5.8%–19.42% in terms of the maximum absolute frequency deviation.

The remainder of this paper is organized as follows. Section II presents a method for identifying the worst-case scenario, while Section III constructs a preventive dispatch model for dealing with the worst frequency deviation. Section IV demonstrates that the proposed preventive dispatch method reduces the maximum absolute frequency deviation. And Section V presents the main conclusions of the paper.

II. Determine the Worst-case Scenario of Frequency Deviation with Adjustable Load

A. Framework

When considering deliberate attacks of adjustable load on the system frequency, we need to formulate the relationship between the power mismatch and the system frequency deviation described by a dynamic frequency response model of the system via differential equations. Currently, a simplified model is commonly used, which directly describes the frequency deviation as a linear function of the power mismatch according to the primary frequency modulation coefficient. It results in modeling error considering the steep frequency fluctuations. Although improved methods have been proposed, there still lacks an efficient method to coordinate the requirements of analytical form and modeling accuracy. Without a proper modeling of frequency deviation, giving the power mismatch, the worst-case scenario cannot be precisely identified.

To address this issue, an analytical relationship between the frequency deviation and power mismatch is formulated in this section. Using the adjustable load p_{d} as a decision variable, the power mismatch Δp_{m} can be directly formulated. Note that the load forecast uncertainty is considered as a component in the change of load. According to the system frequency response model, the frequency deviation Δf caused by the power mismatch can be described as a first-order inertia transfer function, shown as the red block in Fig. 1. The secondary frequency modulation and specific nonlinear links, such as amplitude limiting, are neglected here. The aim is to derive the transfer function in time domain and discretize the function into several segments according to the division of time horizons, such that the discretized expression of frequency deviation can be obtained. Based on the theoretical analysis of the modeling error, it shows that a satisfactory accuracy can be achieved using a computationally tractable expression to approximate the frequency characteristics.

With the analytical relationship between frequency deviation and adjustable load (also power mismatch), the worst-case scenario can be identified by using the frequency deviation as an optimization objective. An optimization model in a MILP form is formulated to achieve this task.

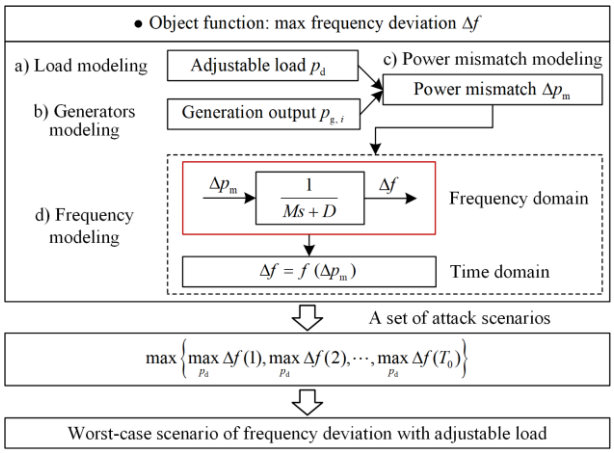

Fig. 1. Outline of the method to determine the worst-case scenario.

B. Expressions Between Power Deviation and System Frequency

A sudden change in load will give rise to unbalanced power, thereby resulting in frequency deviation. In order to ensure sufficient system frequency regulation ability in the case of large power deviation caused by deliberate load attacks, it is necessary to construct the frequency expression Δf as a function of the load adjustment.

The typical model of system frequency response is shown as the red frame in Fig. 1. The governor characteristics are expressed as a first-order inertia element in this model, where Δp_{m} is the difference between load and generation reflecting the imbalance caused by the adjustable load; M is the system moment of inertia; and D is the load damping coefficient. On the basis of the transfer function, the relationship between Δp_{m} and Δf is:

$$\Delta f = \Delta p_{\mathrm{m}} \times \frac{1}{Ms + D} \tag{1}$$

The transfer function of the system can be derived into the time-domain expression of the frequency response by the inverse Laplace transform:

$$\Delta f(t) = \frac{1}{M}\int_0^t \Delta p_{\mathrm{m}}(\tau)\, \mathrm{e}^{\frac{-D}{M}(t-\tau)}\mathrm{d}\tau \tag{2}$$

Equation (2) is the basic continuous-time frequency deviation model, which demonstrates the relationship between the frequency deviation and generation-load power imbalance. However, the integral part exhibits intractable mathematical complexity. To address this problem, a discretization of the integration time horizon [0, t] is used here:

$$[0,t] = [t_0,t_1] \cup [t_1,t_2] \cup \cdots \cup [t_{n-1},t_n] \tag{3}$$

where $t_0 = 0$ and $t_n = t$.

Then, the integral interval can be divided into n segments, as:

$$\Delta f(t) = \frac{1}{M}\left[\begin{array}{l}\int_0^{t_1} \Delta p_{\mathrm{m}}(\tau)\mathrm{e}^{\frac{-D}{M}(t-\tau)}\mathrm{d}\tau + \int_{t_1}^{t_2} \Delta p_{\mathrm{m}}(\tau)\mathrm{e}^{\frac{-D}{M}(t-\tau)}\mathrm{d}\tau + \\ \cdots + \int_{t_{n-1}}^{t} \Delta p_{\mathrm{m}}(\tau)\mathrm{e}^{\frac{-D}{M}(t-\tau)}\mathrm{d}\tau\end{array}\right] = \frac{1}{M}\sum_{i=1}^{n}\int_{t_{i-1}}^{t_i} \Delta p_{\mathrm{m}}(\tau)\mathrm{e}^{\frac{-D}{M}(t-\tau)}\mathrm{d}\tau \tag{4}$$

If the interval is sufficiently small, the integral variable $\Delta p_{\mathrm{m}}(\tau)$ can be regarded as a constant in each interval as $\Delta p(x_i)$, where $x_i \in [t_{i-1}, t_i]$. Equation (4) can be approximated as:

$$\Delta f(t) \approx \Delta f^{\mathrm{new}}(t) = \frac{1}{M}\sum_{i=1}^{n} \Delta p(x_i)\int_{t_{i-1}}^{t} \mathrm{e}^{\frac{-D}{M}(t-\tau)}\mathrm{d}\tau = \frac{1}{D}\sum_{i=1}^{n} \Delta p(x_i)\left(\mathrm{e}^{\frac{-D}{M}(t-t_i)} - \mathrm{e}^{\frac{-D}{M}(t-t_{i-1})}\right) \tag{5}$$

where

$$\int_{t_{i-1}}^{t} \mathrm{e}^{\frac{-D}{M}(t-\tau)}\mathrm{d}\tau = \frac{D}{M}\left(\mathrm{e}^{\frac{-D}{M}(t-t_i)} - \mathrm{e}^{\frac{-D}{M}(t-t_{i-1})}\right) \tag{6}$$

As $t_n = t$, the last item $\mathrm{e}^{\frac{-D}{M}(t-t_n)} = 1$. Equation (5) can be rewritten as:

$$\Delta f^{\mathrm{new}}(t) = \frac{1}{D}\sum_{i=1}^{n-1} \Delta p(x_i)\left(\mathrm{e}^{\frac{-D}{M}(t-t_i)} - \mathrm{e}^{\frac{-D}{M}(t-t_{i-1})}\right) + \frac{1}{D}\Delta p(x_n)\left(1 - \mathrm{e}^{\frac{-D}{M}(t-t_{n-1})}\right) \tag{7}$$

Notably, $\mathrm{e}^{\frac{-D}{M}(t-t_{n-1})}$ is monotone decreasing because of the negative exponent, and its value tends to zero with the increase of $t - t_i$ in certain D and M. Hence, for (7), the former component is approximately zero as the value of $\frac{D}{M}(t - t_i)$ is relatively large in these terms. Equation (7) can be rewritten as:

$$\Delta f^{\mathrm{new}}(t) \approx \frac{1}{D}\Delta p(x_n)\left(1 - \mathrm{e}^{\frac{-D}{M}(t-t_{n-1})}\right) \tag{8}$$

Because $x_n \in [t_{n-1}, t_n]$ and Δp_{m} is discrete with interval K in dispatch model, $\Delta p(x_n)$ is set to $\Delta p_m(t_{n-1})$ and the interval length of $[t_{n-1}, t_n]$ is matching the discrete interval of Δp_{m}. Finally, the analytic frequency expression is obtained by the numerical integral method, as:

$$\Delta f(t) \approx \frac{1}{D}\Delta p_{\mathrm{m}}(t-K)\left(1 - \mathrm{e}^{\frac{-D}{M}K}\right) \tag{9}$$

The frequency deviation is therefore linearly related to power mismatch, and is positively associated with the power mismatch from the previous scheduling moment.

According to the process from continuous-time frequency deviation to discrete formulations, two approximations introduce errors: piecewise constant power mismatch and truncation of historical terms. The former arises from assuming $\Delta p_{\mathrm{m}}(\tau)$ to be constant within each discretization interval, which is associated with the rate of power change. The latter is from the former component of (7), which is approximately zero. For the above sources of error, the choice of the time-step K is a practical way to minimize discretization error. The numerical results in Section IV show that the errors are practically negligible, ensuring the proposed method's reliability for industrial applications.

When the power mismatch is incurred by attacks on the adjustable load, the system frequency will fluctuate.

Based on the frequency deviation described by (9), the worst-case scenario caused by attacks of adjustable load can be identified. The scheduling plan can be adjusted in a timely manner to ensure frequency security accordingly.

C. Determine the Worst-case Scenario

In practical operations of power systems, the system operator is obliged to implement secure and economic dispatch. Considering the potential risk that a large amount of adjustable load may be maliciously controlled, the risk to the power system will be greatly increased. Therefore, this subsection determines the worst-case scenario for the load attack, providing a basic scenario for preventive dispatch.

Based on the analytical frequency model above, the deviation of the adjustable load is taken as the decision variable, and the situation with the largest frequency deviation can be determined.

Suppose T is the total number of scheduling intervals, which is further divided into K number of short intervals to mimic the frequency sampling, while I is the set for generators.

Continuous variable p_{d} is the adjustable load, which is the main optimization variable to determine the worst-case scenario. For generator modeling, continuous variables are the generation output and the dispatched regulation-up/down capacity of generator i, i.e., $\left[p_{\mathrm{g},i}, R_{\mathrm{up/dn},i}\right]$. Continuous variables $\left[\Delta p_{\mathrm{m}}, \Delta p_{\mathrm{sys}}, \Delta p_i\right]$ are the power mismatch of the system, the regulation mileage requirement, and the output adjustment of regulation generators, which are related to the modeling of power mismatch.

The objective is to find the load value that causes the frequency deviation, shown as:

$$\max_{p_{\mathrm{d}}} \Delta f \tag{10}$$

A set of constraints is shown as the following subsections.

1) Load Modeling

$$\sum_{i\in I} p_{\mathrm{g},i}^{t,k} = D^{t,k} + p_{\mathrm{d}}^{t,k}, \quad k=1 \tag{11}$$

$$p_{\mathrm{d}}^{\min} \leqslant p_{\mathrm{d}}^{t,k} \leqslant p_{\mathrm{d}}^{\max} \tag{12}$$

where $p_{\mathrm{g},i}^{t,k}$ is the generation output of generator i in the kth short interval of the tth dispatch interval; $D^{t,k}$ is the basic load of the system in the kth short interval of the tth dispatch interval; $p_{\mathrm{d}}^{t,k}$ is the system adjustable load in the kth short interval of the tth dispatch interval; and $p_{\mathrm{d}}^{\max/\min}$ is the maximum/minimum adjustable load.

Equation (11) is the power balance constraint and the limits to which the adjustable load may be varied are set by the minimum and maximum values in (12).

2) Generator Modeling

$$\begin{cases} 0 \leqslant R_{\mathrm{up},i}^{t} \leqslant \min\left\{r_{\mathrm{up},i}, R_{i,\max,\mathrm{up}}\right\} \\ 0 \leqslant R_{\mathrm{dn},i}^{t} \leqslant \min\left\{r_{\mathrm{dn},i}, R_{i,\max,\mathrm{dn}}\right\} \end{cases} \tag{13}$$

$$\begin{cases} \sum_{i\in I} R_{\mathrm{up},i}^{t} \geqslant R_{\mathrm{up,sys}}^{t} \\ \sum_{i\in I} R_{\mathrm{dn},i}^{t} \geqslant R_{\mathrm{dn,sys}}^{t} \end{cases} \tag{14}$$

$$-r_{\mathrm{dn},i} \leqslant p_{\mathrm{g},i}^{t} - p_{\mathrm{g},i}^{t-1} \leqslant r_{\mathrm{up},i} \tag{15}$$

$$P_{\mathrm{g},i,\min} + R_{\mathrm{dn},i}^{t} \leqslant p_{\mathrm{g},i}^{t} \leqslant P_{\mathrm{g},i,\max} - R_{\mathrm{up},i}^{t} \tag{16}$$

where $R_{\mathrm{up/dn},i}^{t}$ is the dispatched regulation-up/down capacity of generator i in the tth dispatch interval; $R_{i,\max,\mathrm{up/dn}}$ is the maximum available regulation-up/down capacity of generator i; $r_{\mathrm{up/dn},i}$ is the intra-interval ramping-up/down capability of generator i between two short intervals; $R_{\mathrm{up/dn,sys}}^{t}$ is the system regulation-up/down capacity requirement in the tth dispatch interval; and $P_{\mathrm{g},i,\mathrm{max/min}}$ is the maximum/minimum generation output of generator i.

Constrains (13) and (14) ensure that the dispatched regulation capacity is not larger than the maximum capacity of the generator and the sum of the dispatched regulation capacity could meet the system requirement. Constrains (15) and (16) are operational constraints for generators.

3) Power Mismatch Modeling

$$\Delta p_{\mathrm{m}}^{t,k} = \left(D^{t,k} + p_{\mathrm{d}}^{t,k}\right) - \sum_{i\in I} p_{\mathrm{g},i}^{t,k} \tag{17}$$

$$\Delta p_{\mathrm{sys}}^{t,k} = \left(D^{t,k} + p_{\mathrm{d}}^{t,k}\right) - \sum_{i\in I} p_{\mathrm{g},i}^{t,k} - \left[\left(D^{t,k-1} + p_{\mathrm{d}}^{t,k-1}\right) - \sum_{i\in I} p_{\mathrm{g},i}^{t,k-1}\right] = \Delta p_{\mathrm{m}}^{t,k} - \Delta p_{\mathrm{m}}^{t,k-1} \tag{18}$$

$$d - \left(1 - z_{\mathrm{up}}^{t,k}\right)\omega \leqslant \Delta p_{\mathrm{sys}}^{t,k} \leqslant d + z_{\mathrm{up}}^{t,k}\omega \tag{19}$$

$$-d - z_{\mathrm{dn}}^{t,k}\omega \leqslant \Delta p_{\mathrm{sys}}^{t,k} \leqslant -d + \left(1 - z_{\mathrm{dn}}^{t,k}\right)\omega \tag{20}$$

$$p_{\mathrm{g},i}^{t,k} = p_{\mathrm{g},i}^{t,k-1} + \frac{p_{\mathrm{g},i}^{t+1,k} - p_{\mathrm{g},i}^{t,k}}{K} \tag{21}$$

$$p_{\mathrm{g},i}^{t,k} = p_{\mathrm{g},i}^{t,k-1} + \Delta p_{i}^{t,k} \tag{22}$$

$$\Delta p_{\mathrm{sys}}^{t,k} = \sum_{i\in I} \Delta p_{i}^{t,k} \tag{23}$$

where $\Delta p_{\mathrm{m}}^{t,k}$, $\Delta p_{\mathrm{sys}}^{t,k}$, and $\Delta p_{i}^{t,k}$ are the power mismatch of the system, the regulation mileage requirement, and the output adjustment of regulation generator i in the kth short interval of the tth dispatch interval; and ω is a large positive constant [27].

The power mismatch, which is associated with the frequency deviation and causes the regulation generators to adjust to maintain frequency security, is caused by the difference between generation and load, as shown in (17). Regulation mileage refers to the sum of absolute changes in generation output following AGC signals, which is the difference of the continuous power mismatch, as shown in (18). Because the generation output of regulation generators does not change before activating AGC, the mileage requirements are compared with the dead band through (19) and (20) by introducing the integer variables $z_{\text{up/dn}}^{t,k}$. The system regulation and intra-interval generation adjustment are explicitly formulated in a mixed-integer optimization model [28]. For non-regulation generators, the generation output gradually changes to the set points of the next dispatch interval. Hence, it is modeled as a linear ramp in accordance to industrial practice, as shown in (21). For regulation generators, their output will be adjusted based on the previous short interval, as shown in (22) and (23).

Then, a set of attack scenarios to make the maximum frequency deviation can be obtained by the dispatch model formulated in (10)–(23), where (10) is the objective function. The entire adjustable load can be attacked at any time. Among this set of scenarios, the scenario with the largest frequency deviation is the worst-case scenario, as shown in (24). The process of obtaining the set of attack scenarios can be solved in parallel, which greatly accelerates computation speed, decreases computation time and improves computation efficiency.

$$\max\left\{\max_{p_{\text{d}}}\Delta f(1),\max_{p_{\text{d}}}\Delta f(2),\cdots,\max_{p_{\text{d}}}\Delta f(T_0)\right\} \tag{24}$$

where T_0 is the total number of dispatch intervals.

Thus, the worst-case scenario for adjustable load deviations can be determined. The corresponding schedule adjustments to mitigate the resulting frequency threat are addressed in the following section.

III. Preventive Dispatch Against Worst Frequency Deviation

A. Framework

To prevent the potential frequency risk caused by the adjustable load, the generation scheduling needs to be adjusted as well, e.g., more reserves with higher load tracking abilities can be prepared. In the event of power mismatch, the generators are adjusted according to the command from the AGC system. It is evident that different generators exhibit different load tracking abilities [16]. However, existing dispatch model cannot analytically distinguish these differences in generator response to the AGC system. To achieve this, two steps are required, as shown in Fig. 2. First, the allocation of power mismatch to individual generators that mimics the AGC system is required, as reported in recent studies [29]–[31]. Second, the generator ramping behavior after receiving the AGC adjustment command needs to be modeled, to distinguish generators load tracking abilities.

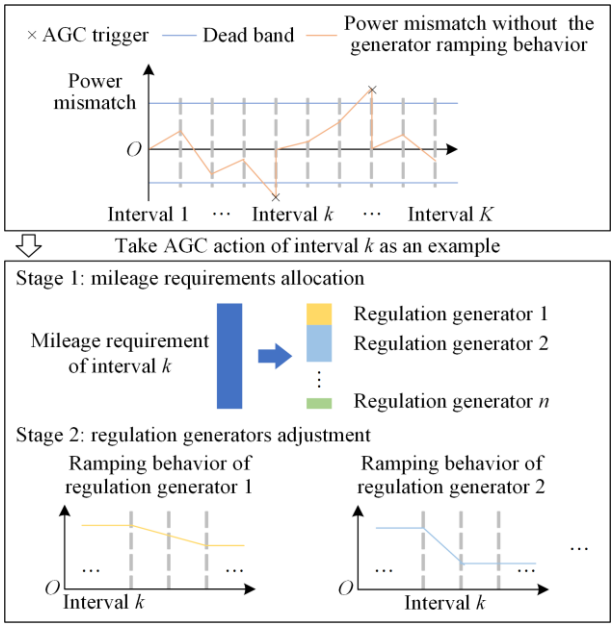

Fig. 2. Generators are adjusted to deal with the power mismatch.

After the modeling of generator actions, a preventive dispatch model against adjustable load attacks on system frequency can be formulated. The frequency deviation can be directly constrained to ensure safe system operation.

B. Modeling of the AGC Action for Frequency Regulation

First, the modeling for the allocation of power mismatch to individual generators is presented. Because of the difference in generator regulation-up and regulation-down, it is necessary to distinguish between regulation-up and regulation-down requirements. According to (17)–(20), the mileage requirements can be further divided into regulation-up requirements and regulation-down requirements, as shown in (25) and (26). The solving process is accelerated by the strategies that regulation-up requirements and regulation-down requirements do not come at the same time, as shown in (27).

$$\begin{cases}\Delta p_{\text{sys}}^{t,k}-\left(1-z_{\text{up}}^{t,k}\right)\omega\leqslant\Delta p_{\text{up}}^{t,k}\leqslant z_{\text{up}}^{t,k}\omega\\ -z_{\text{up}}^{t,k}\omega\leqslant\Delta p_{\text{up}}^{t,k}\leqslant\Delta p_{\text{sys}}^{t,k}+\left(1-z_{\text{up}}^{t,k}\right)\omega\end{cases} \tag{25}$$

$$\begin{cases}-\Delta p_{\text{sys}}^{t,k}-\left(1-z_{\text{dn}}^{t,k}\right)\omega\leqslant\Delta p_{\text{dn}}^{t,k}\leqslant z_{\text{dn}}^{t,k}\omega\\ -z_{\text{dn}}^{t,k}\omega\leqslant\Delta p_{\text{dn}}^{t,k}\leqslant-\Delta p_{\text{sys}}^{t,k}+\left(1-z_{\text{dn}}^{t,k}\right)\omega\end{cases} \tag{26}$$

$$z_{\text{up}}^{t,k}+z_{\text{dn}}^{t,k}\leqslant 1 \tag{27}$$

where $\Delta p_{\text{up/dn}}^{t,k}$ is system regulation-up/down requirements in the kth short interval of the tth dispatch interval.

The mileage requirements are allocated to each regulation generator by (23).

The above work refers to [28]. In fact, the generators cannot immediately reach the assigned mileage requirements. The response time of regulation generation to reach the allocated adjustment cannot be neglected because of its capability of ramping up to full output in tens of seconds, which is comparable to the AGC timescale. Hence, the next stage is the modeling of generator ramping behavior after receiving the AGC adjustment command, which is one of the contributions of this paper.

Different from the generators climbing constraint (15), the AGC adjustment command received by each generator needs to be executed as quickly as possible. For example, at t, Δp_i is allocated to generator i, as shown in Fig. 3.

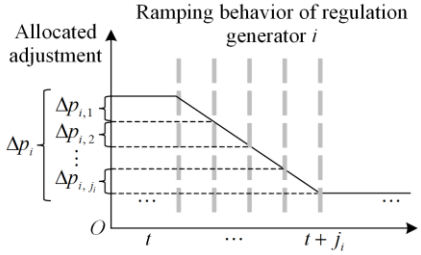

Fig. 3. The ramping behavior of regulation generator i at t.

The generator needs a certain response time to reach the distribution point. Δp_i is divided into segments such as $\Delta p_{i,1}, \Delta p_{i,2}, \cdots, \Delta p_{i,j_i}$, where j_i is the number of segments, shown as:

$$\Delta p_i = \sum_{j=1}^{j_i} \Delta p_{i,j} \tag{28}$$

Assume the generator ramps linearly, which means that the adjusted power allocated to the generator is evenly distributed over the following periods, where $\Delta p_{i,1} = \Delta p_{i,2} = \cdots = \Delta p_{i,j_i}$ Hence, equation (28) can be rewritten as:

$$\Delta p_{i,j} = \frac{1}{j_i} \Delta p_i \tag{29}$$

where j_i is associated with the adjustment capacity of each generator, with smaller values indicating faster ramping and shorter adjustment times.

Besides, the generator is adjusted only when it is assigned an adjustment amount and the previous adjustment amount has been completed. Hence, integer variables $z_{\text{g,up},i}^{t,k}$ and $z_{\text{g,dn},i}^{t,k}$ are introduced to distinguish whether generator i is adjusted to balance the intra-interval fluctuations. If generator i provides the regulation, $z_{\text{g,up/dn},i}^{t,k}$ will be constrained to 1; otherwise, it will be constrained to 0.

$$\Delta p_{\text{up/dn}}^{t,k} = \sum_{i \in I} \Delta p_{\text{up/dn},i}^{t,k} \tag{30}$$

$$\begin{cases} \Delta p_{\text{up/dn,i}}^{t,k} - \left(1 - z_{\text{g,up/dn},i}^{t,k}\right)\omega \leqslant \Delta p_{\text{up/dn},i}^{t,k} \leqslant z_{\text{g,up/dn},i}^{t,k}\omega \\ -z_{\text{g,up/dn},i}^{t,k}\omega \leqslant \Delta p_{\text{up/dn},i}^{t,k} \leqslant \Delta p_{\text{up/dn,i}}^{t,k} + \left(1 - z_{\text{g,up/dn},i}^{t,k}\right)\omega \end{cases} \tag{31}$$

$$\Delta p_i^{t,k} = \Delta p_{\text{up},i}^{t,k} + \Delta p_{\text{dn},i}^{t,k} = \sum_{j=0}^{j_i - 1} \frac{1}{j_i} \Delta p_{i,j}^{t,k-j} \tag{32}$$

$$\sum_{k=t_i}^{t_i + j_i} z_{\text{g,up/dn},i}^{t,k} \leqslant 1 \tag{33}$$

where $\Delta p_{\text{up/dn},i}^{t,k}$ is the allocated regulation-up/down requirements of generator i in the kth short interval of the tth dispatch interval; $\Delta p_{i,j}^{t,k-j}$ is the output adjustment of regulation generator i in the $(k-j)$th short interval of the tth dispatch interval.

The generator ramping behavior after receiving the AGC adjustment command is modeled. Hence, when the power difference is larger than the dead band and the generator has the ability to adjust, equation (22) is transferred to:

$$p_{\text{g},i}^{t,k} = p_{\text{g},i}^{t,k-1} + \Delta p_{i,j}^{t,k} \tag{33}$$

Combined with (23), mileage requirements are optimally allocated to each generator. This ensures that the AGC generators with higher ramping capability are assigned larger mileage requirements, thereby maintaining frequency stability following AGC command. Otherwise, insufficient ramping response would aggravate power imbalance, resulting in higher regulation costs and undermining the objectives of the dispatch.

Finally, equations (25)–(27) and (30)–(34) present the modeling of generators considering the difference in load tracking ability. The model supports the dispatch of fast generators to prepare for load attack, thus ensuring frequency security.

C. Formulations of the Preventive Dispatch Model

After modeling the frequency and AGC generator behaviors, the preventive dispatch model can be established under the attack of adjustable load.

The objective is to minimize the total operating costs. The three items in (35) are the energy costs, regulation capacity costs, and regulation mileage costs successively.

$$\min \sum_{t \in T} \sum_{k \in K} \sum_{i \in I} \left[C_{\text{g},i} p_{\text{g},i}^{t,k} + \left(C_{\text{up},i} R_{\text{up},i}^{t} + C_{\text{dn},i} R_{\text{dn},i}^{t} \right) + C_{\text{m},i} \Delta p_i^{t,k} \right],$$

$$\text{s.t.} \begin{cases} \text{power balance constraint: (11)} \\ \text{generator constraints: (13)–(16)} \\ \text{power mismatch constraints:} \\ \text{(17)–(21), (25)–(27), (30)–(34)} \\ \text{frequency constraints: (9), } \Delta f^{\min} \leqslant \Delta f^{t,k} \leqslant \Delta f^{\max} \end{cases} \tag{35}$$

where $C_{g,i}$, $C_{up/dn,i}$, and $C_{m,i}$ are the energy cost, regulation-up/down capacity cost, and regulation mileage cost of generator i, respectively; and $\Delta f^{max/min}$ is the maximum/minimum frequency deviation.

As the worst-case scenario of frequency deviation with adjustable load has been determined, the adjustable load is set. Hence, according to loading modeling, only the power balance constraint is preserved.

Finally, the preventive dispatch against the worst frequency deviation is formulated by (35). For the convenience of computing, a linear objective function is used. The general framework is shown in Fig. 4. As all constraints are linear, the models established in this paper are MILP models, which can be easily solved. The computational time of the dispatch model is crucial for practical applicability of the proposed method. Because of the fewer time intervals and the non-complicated problem, the proposed MILP model achieves good computational performance in the case studies. It is obvious that with the increase in time resolution and number of generators, leading to an increase in constraints accordingly, computational challenges arise. For larger systems, calculation times may be prohibitively long. Several approaches can be adopted to address this issue; for example, the root relaxation of the dispatch problem is often close to a feasible solution, as observed in many discrete dispatch problems.

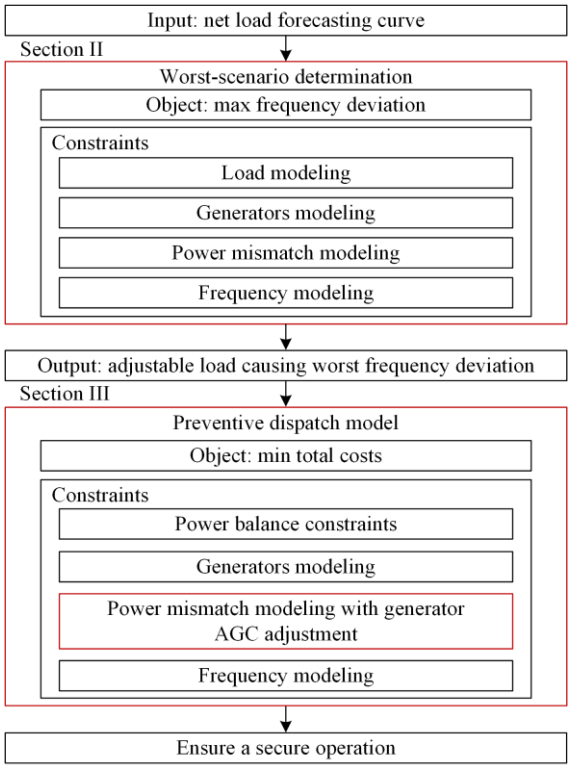

Fig. 4. Framework of the proposed preventive dispatch method.

It should be noted that the inertia of the whole system is considered, but the inertia of a single generator is not analyzed in detail. Hence, the delay factor of the generator after receiving the AGC control signal is not considered, whereas the ramping process of the generator is modeled. While the linear ramping model simplifies computation and enables accessible optimization, it has inherent limitations in capturing real-world generator dynamics. For example, neglecting nonlinear ramping may cause temporary mismatches between AGC commands and actual output. Besides, high penetration of renewables amplifies power mismatch volatility. Linear models may fail to coordinate fast-ramping generators with slow-ramping units effectively. Refine the generator inertia difference, delay mechanism and nonlinear ramping can be explored in subsequent research.

In addition, the model assumes static prices according to (35), indicating constant price during dispatch, so it fails to capture dynamic market mechanisms or incentive structures that could reshape generator behaviors. Varying economic incentives profoundly influence resource allocation and frequency stability, which can also be incorporated into future research.

IV. Case Study

The effectiveness and accuracy of the proposed preventive dispatch model considering the attack of adjustable load on power system frequency is verified on the IEEE30-bus system and a utility system. To ensure sufficient regulation capacities are reserved, the system regulation-up/down capacity requirement of each dispatch interval is set to 5% of the peak load in the interval. For simplicity, all generators submit the same cost for regulation-up/down services, and dispatch is implemented every 5 min for six dispatch intervals (30 min. Each dispatch interval contains 10 short intervals (each short interval is 30 s).

Three methods are compared to demonstrate the effectiveness of the proposed preventive model:

1) M1: the proposed preventive dispatch model with the modeling of AGC action for frequency regulation considering the attack of adjustable load on the power system frequency;

2) M2: current dispatch model without the AGC action for frequency regulation;

3) M3: current dispatch model without taking any measures after the attack of adjustable load.

The hardware environment used in this paper is a personal computer with an Intel(R) Core(TM) i7-8700K CPU@3.70GHz 32.0 GB RAM. The optimization model is solved on the software platform MATLAB using GUROBI 11.0.0 as the solver for the MILP problem [32]. The total execution time for solving the problem in the IEEE30-bus system is approximately 1.0811 s, while in the practical utility system, it is 1.1424 s, meeting the practical requirements.

A. IEEE30-bus System

The IEEE30-bus system is first used to test the proposed model. The total system load is the sum of the base load and the adjustable load. In this case, the adjustable load range is set to 0 to 25% of the maximum generator output, which does not affect the effectiveness of the proposed method. The parameters of the generators in the IEEE30-bus system are summarized in [33], with a total of 6 generators being contained in this case.

1) Worst-case Scenario Determination

Before the worst-case scenario is confirmed, the effectiveness of the characterization of frequency should be verified. To validate the effectiveness of the established expressions (9) for power deviation and system frequency, a continuous set of power deviations is randomly generated. Compared with the time-domain simulation, which serves as the actual frequency, the frequency deviations obtained by (9) are shown in Fig. 5. The cumulative error is 8.09×10^{-4}.

Taking the 7th dispatch point as an example for (7)–(9), the value of each component of (7) is shown in Fig. 6, and the results for different values of K are compared. Obviously, the former components are approximately 0. The actual frequency deviation is 0.0454 Hz, which is near the last component. It should be noted that each short dispatch interval is 30 s in this case. For the value of K, it is advisable to maintain consistency with the dispatch interval, as it results in fewer fitting errors and is also convenient.

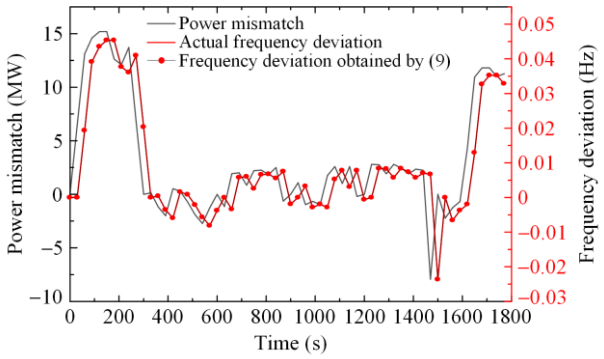

Fig. 5. Frequency deviations and power mismatch.

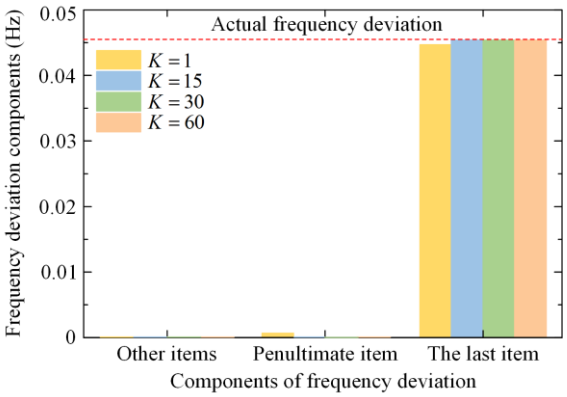

Fig. 6. Each component of Eq. (7) for different K.

It is observed that Eq. (9) can obtain frequency results highly similar to those obtained by time-domain simulation. Therefore, the proposed frequency constraint, with a tolerable loss of accuracy, can be easily incorporated into commonly used scheduling models.

The worst-case scenario of frequency deviation with adjustable load is obtained by optimization based on M3. A set of attack scenarios can be obtained by taking the maximum frequency deviation of each scheduling moment in the scheduling period as the objective function. In this set of scenarios, the scenario with the largest frequency deviation is the worst-case scenario.

Maximum frequency deviations with/without attack for each scenario are shown in Fig. 7. It is observed that the worst attack scenario appears in the 20th dispatch point (as illustrated by the red circle in Fig. 7). Hence, the worst-case scenario is determined, and the frequency deviation is shown in Fig. 7.

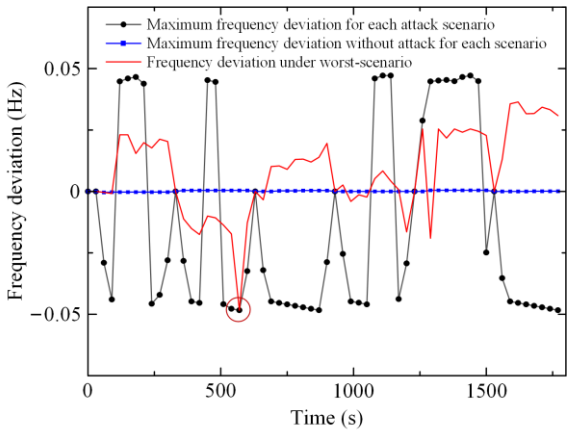

Fig. 1. Frequency deviation in each scenario for the IEEE30-bus system.

The load curves in the worst-case scenario before and after the attack of adjustable load are described in Fig. 8. The frequency deviation is compared in Table I. It can be seen that the attack of adjustable load leads to unsafe frequency changes. In the following sections, the comparisons among the different methods are performed under the worst-case scenario.

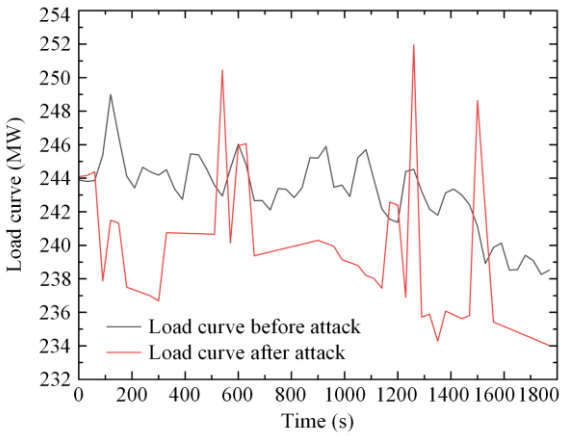

Fig. 8. Load curve for the IEEE30-bus system before and after the attack of adjustable load.

TABLE I
COMPARISON OF FREQUENCY DEVIATIONS AND TOTAL OPERATING COSTS

Index	Before the attack of adjustable load	After the attack of adjustable load
The range of Δf (Hz)	$(-3.6080\times10^{-4}, 4.8005\times10^{-4})$	(−0.0484, 0.0364)

2) Analysis of the Dispatch Results

The superiority of the proposed model (M1) can be seen in the improvement of the system frequency performance, as shown in Table II and Table III.

TABLE II
FREQUENCY PERFORMANCE OF M1, M2 AND M3 IN IEEE30-BUS SYSTEM

	M1	M2	M3
The range of Δf (Hz)	(−0.0390, 0.0198)	(−0.0414, 0.0262)	(−0.0484, 0.0364)
The maximum absolute frequency deviation (Hz)	0.0390	0.0414	0.0484
The standard deviation of Δf (Hz)	0.011 36	0.013 16	0.014 97
Root mean square error of Δf	0.011 36	0.013 24	0.014 98

TABLE III
PERFORMANCE IMPROVEMENT OF M1 COMPARED WITH M2 AND M3 (%)

Performance improvement	Compared with M2	Compared with M3
The range of Δf	13.02	14.78
The maximum absolute frequency deviation	5.80	19.42
The standard deviation of Δf	13.68	24.11
Root mean square error of Δf	14.20	24.17

It can be observed that M1 exhibits superior frequency performance, as reflected by improvements in the range of Δf, the maximum absolute frequency deviation, the standard deviation, and root mean square error of Δf. Specifically, these metrics are improved by 13.02%, 5.80%, 13.68%, and 14.20%, respectively, compared with M2. This indicates that frequency deviations can be kept smaller and more stable by implementing the proposed preventive dispatch model. This improvement arises because, following AGC adjustment commands, generators with faster ramping capability respond more rapidly, thereby enhancing overall frequency stability.

For instance, the results show that generator 1 and generator 4 are regulation generators. Actual generation outputs of generator 1 and generator 4 obtained by M1 and M2 are shown in Fig. 9, with generator 1 exhibiting better climbing performance than generator 4. The regulation-down mileage requirement is 0.77 MW at the dispatch interval indicated by the blue circle in Fig. 9. In M2, generator 4 is dispatched to provide the regulation-down service as its cost is lower than generator 1. By comparison, only generator 1 is dispatched in M1 as it is faster than generator 4. Correspondingly, Δf is 0.01 829 Hz in M1 and 0.02 621 Hz in M2.

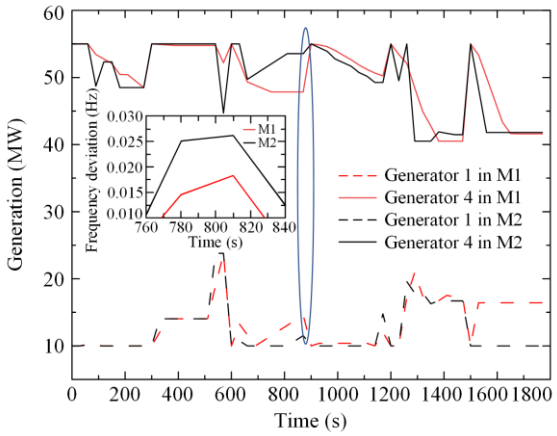

Fig. 9. Actual generation output of generator 1 and generator 4 obtained by M1 and M2.

In summary, benefiting from the modeling of the frequency regulation behaviors, the proposed dispatch method can maintain frequency security under the attack of adjustable load.

B. Practical 661-bus Utility System

To validate the scalability of the proposed method, the performance of the proposed method is tested on a practical utility system. This system is based on a provincial power system in China. It consists of 661 buses and 48 generators. Details of this practical system can be found in [33].

Maximum frequency deviations with different attacks for each scenario are shown in Fig. 10. It is observed that the worst attack scenario is determined as the 41st dispatch point (as illustrated by the red circle in Fig. 10).

The load curves before and after the attack of adjustable load are described in Fig. 11. The red line shows the load curve in the worst-case scenario.

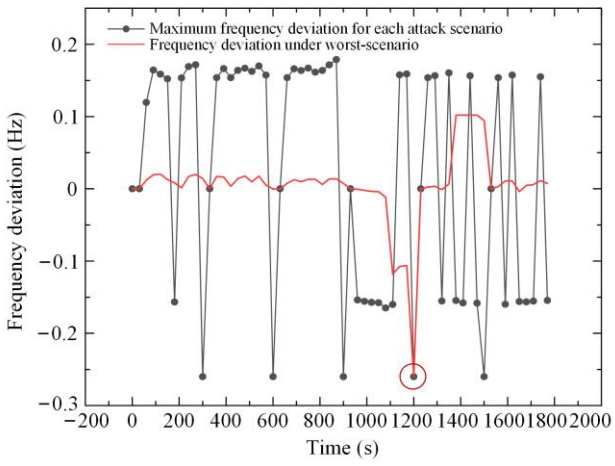

Fig. 10. Frequency deviation in each scenario for the practical 661-bus utility system.

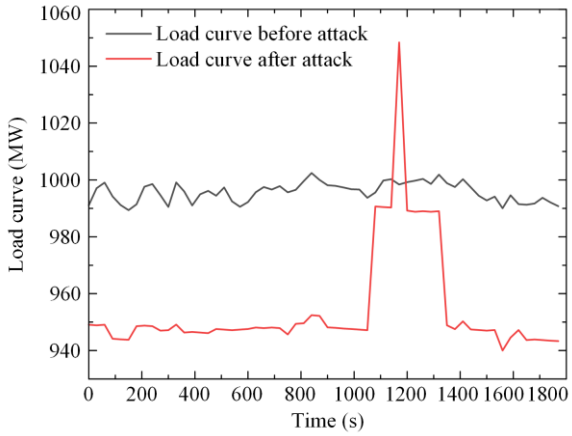

Fig. 11. Load curve for the practical 661-bus utility system before and after the attack of adjustable load.

Comparing M1 with M2, the frequency deviation indices are shown in Table IV. It can be seen that the proposed method improves the frequency performance, resulting in smaller maximum absolute frequency deviation with a 6.8% improvement compared with M2. The reason is similar to that illustrated in Section IV.A.2).

TABLE IV
FREQUENCY PERFORMANCE OF M1 AND M2 IN THE PRACTICAL 661-BUS UTILITY SYSTEM

	M1	M2	Performance improvement
The range of Δf (Hz)	(−0.0888, 0.0468)	(−0.0953, 0.0421)	1.34%
The maximum absolute frequency deviation (Hz)	0.0888	0.0953	6.80%
The standard deviation of Δf (Hz)	0.0234	0.0249	5.88%
Root mean square error of Δf	0.0234	0.0249	5.88%

V. CONCLUSION AND FURTHER DISCUSSION

In this paper, a preventive dispatch method against attacks of adjustable load on power system frequency is presented. First, the relationship between power fluctuation and frequency deviation is established by deriving the transfer function. Based on this, the worst-case scenario for the attack of adjustable load is determined. To adjust the generation schedule against such frequency threat, the intra-interval frequency regulation behaviors of generators are modeled. Subsequently, the preventive dispatch model, which is a MILP model, is introduced and can be solved for straight away. The results of the case study show that the proposed method is reliable and improves system frequency security. While the foundational model is classical, its novel application to worst-case scenarios and scalable implementation in real-world systems show its technical and practical significance.

A thorough comprehension of the risk posed by adjustable loads to power systems can offer guidance for enhancing the operational strategy of power systems. The presence of renewable energy sources and the uncertainty associated with their power will affect the frequency deviation in the case of an attack of adjustable load. The proposed preventive dispatch method is inherently designed to address time-varying power mismatches, making it adaptable to systems with high renewable penetration. However, renewable energy fluctuations may have different statistical properties, such as higher frequency and magnitude, which may require to adjust model parameters or add additional constraints. Further research could enable more precise prediction of the impact of adjustable load attack on power system frequency and account for additional uncertainties, thereby establishing more realistic worst-case scenarios. Combined with the research presented in this paper, the security and robustness of the power system can be enhanced, and the risk of frequency attack by the adjustable load can be well-controlled.

ACKNOWLEDGMENT

Not applicable.

AUTHORS' CONTRIBUTIONS

Yuan Zhang: writing original draft, software, methodology, and conceptualization. Mingxu Xiang: writing review, editing, and visualization. Zhengwen Huang: writing review and editing. Zhifang Yang: writing review, editing, and supervision. All authors read and approved the final manuscript.

FUNDING

This work is supported by the National Natural Science Foundation of China (No. 52307082 and No. W2421081).

AVAILABILITY OF DATA AND MATERIALS

Not applicable.

DECLARATIONS

Competing interests: The authors declare that they have no known competing financial interests or personal relationships that could have appeared to influence the work reported in this article.

AUTHORS' INFORMATION

Yuan Zhang received the B.S. degree in electrical engineering and automation from Chongqing University, Chongqing, China, in 2021 and she is currently working toward the Ph.D. degree in electrical engineering from

Chongqing University. Her research interests include power system operation and electricity market.

Mingxu Xiang received the Ph.D. degree in electrical engineering from Chongqing University, Chongqing, China, in 2022. He is currently an assistant research fellow with Chongqing University. His research interests include power system operation and electricity market.

Zhengwen Huang received the Ph.D. degree from the Department of Electronic and Computer Engineering, Brunel University London, Uxbridge, UK, in 2014. He is currently the UK principal investigator of the Artificial Intelligence and Systems Optimization Team at the Brunel-CQUPT Joint Innovation Centre, and a lecturer as well as a senior research fellow at the Department of Electronic and Electrical Engineering, College of Engineering, Design & Physical Sciences, Brunel University London, Uxbridge, UK. His current research interests include evolutionary algorithms (gene expression programming and genetic programming) and data engineering.

Zhifang Yang received the Ph.D. degree in electrical engineering from Tsinghua University, Beijing, China, in 2018. He is currently a professor with Chongqing University. His research interests include power system optimization and electricity market.

REFERENCES

[1] C. W. Gellings, "The concept of demand-side management for electric utilities," *Proceedings of the IEEE*, vol. 73, no. 10, pp. 1468-1470, Oct. 1985.

[2] C. Li, Z. Yan, and Y. Yao *et al.*, "Coordinated low-carbon dispatching on source-demand side for integrated electricity-gas system based on integrated demand response exchange," *IEEE Transactions on Power Systems*, vol. 39, no. 1, pp. 1287-1303, Jan. 2024.

[3] J. Ma and B. Venkatesh, "Integrating net benefits test for demand response into optimal power flow formulation," *IEEE Transactions on Power Systems*, vol. 36, no. 2, pp. 1362-1372, Mar. 2021.

[4] J.-K. Kim, S. Lee, and J.-S. Kim *et al.*, "The need for modeling the impact of behind-the-meter generation trip on primary frequency response through operational experiences in Korea power system," *IEEE Transactions on Power Systems*, vol. 37, no. 2, pp. 1661-1664, Mar. 2022.

[5] Y. Zhang, V. V. G. Krishnan, and J. Pi *et al.*, "Cyber physical security analytics for transactive energy systems," *IEEE Transactions on Smart Grid*, vol. 11, no. 2, pp. 931-941, Mar. 2020.

[6] X. Liu, S. Sun, and Y. Wang *et al.*, "Modeling and detection of false data injection attacks in cyber-physical distribution system with load aggregator interaction," *Sustainable Energy, Grids and Networks*, vol. 40, Dec. 2024.

[7] M. A. Sayed, M. Ghafouri, and R. Atallah *et al.*, "Grid chaos: an uncertainty-conscious robust dynamic EV load-altering attack strategy on power grid stability," *Applied Energy*, vol. 363, Jun. 2024.

[8] A. R. Coffman, Z. Guo, and P. Barooah, "Characterizing capacity of flexible loads for providing grid support," *IEEE Transactions on Power Systems*, vol. 36, no. 3, pp. 2428-2437, May 2021.

[9] H. Liu, K. Huang, and Y. Yang *et al.*, "Real-time vehicle-to-grid control for frequency regulation with high frequency regulating signal," *Protection and Control of Modern Power Systems*, vol. 3, no. 2, pp. 1-8, Apr. 2018.

[10] P. Yan, Z. Yang, and W. Lin *et al.*, "Optimal configuration of intelligent power switches considering multi-dimensional emergency load regulation objectives," *Power System Protection and Control*, vol. 53, no. 22, pp. 162-174, Nov. 2025 (in Chinese).

[11] Z. Bao, W. Qiu, and L. Wu *et al.*, "Optimal multi-timescale demand side scheduling considering dynamic scenarios of electricity demand," *IEEE Transactions on Smart Grid*, vol. 10, no. 3, pp. 2428-2439, May 2019.

[12] S. Soltan, P. Mittal, and H. V. Poor, "BlackIoT: IoT botnet of high wattage devices can disrupt the power grid," in *Proceedings of the 27th USENIX Security Symposium*, Baltimore, USA, Aug. 2018, pp. 15-32.

[13] W. Mo, K. Ye, and Y. Chen *et al.*, "Frequency stability challenges and countermeasures in typical isolated synchronous power grids with high penetration of renewable energy (part II)," *Power System Protection and Control*, vol. 53, no. 18, pp. 179-187, Sep. 2025 (in Chinese).

[14] Y. Huang, X. Wang, and H. Zhang *et al.*, "Improvement of simplified primary frequency regulation model for thermal power units and analytical calculation of power system frequency security constraints," *Power System Protection and Control*, vol. 53, no. 15, pp. 36-47, Aug. 2025 (in Chinese).

[15] G. Cai, S. Zhou, and C. Liu *et al.*, "Hierarchical under frequency load shedding scheme for inter-connected power systems," *Protection and Control of Modern Power Systems*, vol. 8, no. 2, pp. 1-12, Apr. 2023.

[16] H. Chávez, R. Baldick, and S. Sharma, "Governor rate-constrained OPF for primary frequency control adequacy," *IEEE Transactions on Power Systems*, vol. 29, no. 3, pp. 1473-1480, May 2014.

[17] F. Teng, V. Trovato, and G. Strbac, "Stochastic scheduling with inertia-dependent fast frequency response requirements," *IEEE Transactions on Power Systems*, vol. 31, no. 2, pp. 1557-1566, Mar. 2016.

[18] Y. Meng, X. Li, and X. Liu *et al.*, "A control strategy for battery energy storage systems participating in primary frequency control considering the disturbance type," *IEEE Access*, vol. 9, pp. 102004-102018, Jul. 2021.

[19] D. Liu, Q. Yang, and Y. Chen *et al.*, "Optimal parameters and placement of hybrid energy storage systems for frequency stability improvement," *Protection and Control of Modern Power Systems*, vol. 10, no. 2, pp. 40-53, Mar. 2025.

[20] A. M. Nakiganda, S. Dehghan, and U. Markovic *et al.*, "A stochastic-robust approach for resilient microgrid investment planning under static and transient islanding security constraints," *IEEE Transactions on Smart Grid*, vol. 13, no. 3, pp. 1774-1788, May 2022.

[21] W. Yan, R. Zhao, and X. Zhao *et al.*, "Dynamic optimization model of AGC strategy under CPS for interconnected power system," *International Review of Electrical Engineering*, vol. 7, no. 5, pp. 5733-5743, Sep. 2012.

[22] G. Zhang, E. Ela, and Q. Wang, "Market scheduling and pricing for primary and secondary frequency reserve," *IEEE Transactions on Power Systems*, vol. 34, no. 4, pp. 2914-2924, Jul. 2019.

[23] Y. Yang, J. C.-H. Peng, and Z.-S. Ye, "A market clearing mechanism considering primary frequency response rate," *IEEE Transactions on Power Systems*, vol. 36, no. 6, pp. 5952-5955, Nov. 2021.

[24] J. P. Deane, G. Drayton, and B. P. Ó Gallachóir, "The impact of sub-hourly modelling in power systems with significant levels of renewable generation," *Applied Energy*, vol. 113, pp. 152-158, Jan. 2014.

[25] M. Zhang, Z. Yang, and W. Lin *et al.*, "Enhancing economics of power systems through fast unit commitment with high time resolution," *Applied Energy*, vol. 281, Jan. 2021.

[26] R. Philipsen, G. Morales-España, and M. de Weerdt *et al.*, "Trading power instead of energy in day-ahead electricity markets," *Applied Energy*, vol. 233, pp. 802-15, Jan. 2019.

[27] L. Xu, C. Dou, and D. Yue *et al.*, "Cyber-physical-transportation system based co-design of charging pricing and frequency regulation control for EVs in multi-market," *Protection and Control of Modern Power Systems*, vol. 10, no. 6, pp. 1-14, Nov. 2025.

[28] M. Xiang, Z. Yang, and J. Yu *et al.*, "Real-time dispatch with secondary frequency regulation: a pathway to consider intra-interval fluctuations," *IEEE Systems Journal*, vol. 16, no. 4, pp. 5556-5567, Dec. 2022.

[29] Z. Wang, J. Zhong, and J. Li, "Design of performance-based frequency regulation market and its implementations in real-time operation," *International Journal of Electrical Power & Energy Systems*, vol. 87, pp. 187-197, May 2017.

[30] O. Mégel, T. Liu, and D. J. Hill *et al.*, "Distributed secondary frequency control algorithm considering storage efficiency," *IEEE Transactions on Smart Grid*, vol. 9, no. 6, pp. 6214-6228, Nov. 2018.

[31] A. Sadeghi-Mobarakeh and H. Mohsenian-Rad, "Optimal bidding in performance-based regulation markets: an MPEC analysis with system dynamics," *IEEE Transactions on Power Systems*, vol. 32, no. 2, pp. 1282-1292, Mar. 2017.

[32] Gurobi-11.0-Data-Sheet (2024, Jun. 2). [Online]. Available: https://p1.aprimocdn.net/gurobi/66ff8913-30b2-4e67-9a91-b0c80132a5eb/originalfile/Gurobi-11.0-Data-Sheet.pdf

[33] Data Source for Preventive Dispatch (2024, Sep. 26). [Online]. Available: https://github.com/1999YUAN/Data-source-for-Preventive-Dispatch